ADVANCED FUNCTIONAL MATERIALS
www.afm-journal.de

Synergistic Improvement of Actuation Properties with Compatibilized High Permittivity Filler

Sebastian Risse, Björn Kussmaul, Hartmut Krüger, and Guggi Kofod*

Electroactive polymers can be used for actuators with many desirable features, including high electromechanical energy density, low weight, compactness, direct voltage control, and complete silence during actuation. These features may enable personalized robotics with much higher ability to delicately manipulate their surroundings than can be achieved with currently available actuators; however, much work is still necessary to enhance the electroactive materials. Electric field-driven actuator materials are improved by an increase in permittivity and by a reduction in stiffness. Here, a synergistic enhancement method based on a macromolecular plasticizing filler molecule with a combination of both high dipole moment and compatibilizer moieties, synthesized to simultaneously ensure improvement of electromechanical properties and compatibility with the host matrix is presented. Measurements show an 85% increase in permittivity combined with 290% reduction in mechanical stiffness. NMR measurements confirm the structure of the filler while DSC measurements confirm that it is compatible with the host matrix at all the mixture ratios investigated. Actuation strain measurements in the pure shear configuration display an increase in sensitivity to the electrical field of more than 450%, confirming that the filler molecule does not only improve dielectric and mechanical properties, it also leads to a synergistic enhancement of actuation properties by simple means.

1. Introduction

Electroactive polymers belong to the group of smart materials which respond to an electrical stimulus by undergoing large deformations.[1] Polymers have several advantages compared to other actuator technologies, including ease of processing and a broad range of opportunities for property manipulation. Of the many types of either ionic or electronic actuation polymers, the dielectric elastomer actuators possess all of the properties that make electroactive polymers exciting for applications, for instance, low material costs, light weight, scalability, direct voltage control, noiseless performance, shock tolerance, and high power/weight ratios. Because of this unique combination of properties, DEAs are often referred to as "artificial muscles". Several applications based on these properties are currently finding their way into practical usage.[2–5]

Dielectric elastomer actuators (DEAs) are soft capacitors with compliant electrodes, which can achieve large strains under the influence of an electrical field.[5–7] Their actuation properties are determined mainly by two material characteristics, the stiffness and the dielectric properties, quantified to leading order by the Young's modulus Y and the real permittivity ε', respectively. Just as important is the electrical breakdown strength E_B, which limits the ultimate actuation voltage, and is influenced by mechanical stiffness and permittivity,[8,9] as well as factors such as impurities and defects. For most applications where high electromechanical response or lower activation voltage is sought, materials with low stiffness and high permittivity as well as high electrical breakdown fields are desired. Many special applications based on DEAs have been realized, exploiting the large flexibility in design made possible by this technology. Examples are an arm-wrestling robot,[10] a tunable array of soft polydimethylsiloxane (PDMS) lenses,[11] a hydrostatically coupled DEA,[12] a tunable diffractive transmission grating,[13] a swimming blimp with large area DEAs,[14] a tunable elastomer laser,[15] miniaturized pumps,[16] and optical adjustment actuators.[17,18] All these applications have been realized within the last five years. Material improvements are the key enabler for further progress in the field of DEAs, aiming to raise the energy density and lower the operating voltage. Practical approaches are sought that will make the selection of materials with optimal properties for given application as simple as opening a catalogue, while being compatible with practical processing methods.

The use of composites and nanocomposites has been investigated extensively for this purpose, and several methods were found to have an impact on the electromechanical response. The use of conducting nanoparticles in an insulating matrix exploits that permittivity can increase divergently near the percolation threshold; however, the drop in electrical breakdown strength appears to rule out practical usage.[19] Insulating metal oxide particles with high permittivity enables a direct adjustment of the dielectric properties,[20,21] and when the nanoparticles are

S. Risse, Dr. G. Kofod
University of Potsdam
Institute of Physics and Astronomy
Applied Condensed-Matter Physics
Karl-Liebknecht-Str. 24/25, 14476 Potsdam, Germany
E-mail: Sebastian.Risse@uni-potsdam.de
B. Kussmaul, Dr. H. Krüger
Fraunhofer Institute for Applied Polymer Research
Geiselbergstr. 69, 14476 Potsdam, Germany

DOI: 10.1002/adfm.201200320

coated with suitable surface modifying molecules, a high degree of compatibility between matrix and particle is possible.[22] However, these approaches all share the disadvantages that the stiffness of the material increases, that agglomeration can occur, and that the interface between the high permittivity particle and the low permittivity matrix triggers high losses due to universal relaxation.[23] Polymer blending of conducting polymers with insulating elastomer matrices also leads to improvements.[24] Conductive polymers can also be chemically grafted to the elastomer backbone, leading to encapsulated conducting nanoparticles[25] or to encapsulated conducting polymer chains.[22] Finally, it was recently shown that strong organic dipoles can be linked to silicones.[26,27]

Here, a molecular filler is constructed from a reactive silicone molecule which is normally used as cross-linker in the formation of the silicone elastomer network. The reactive methylhydrosiloxane sites of the cross-linking molecules are functionalized with dipole or compatibilizing units, in this case allyl cyanide and allyltrimethylsilane side-groups, respectively. The allyl cyanide is among the highest dipole moments and could lead to precipitation; however, this effect is countered by the allyltrimethylsilane group. During the synthesis, the relative amounts of cyanide dipole to trimethylsilane compatibilizer are chosen to be as high as possible, as determined by the avoidance of phase separation between the reactants in the non-polar solvent (see the Experimental Section). Allyl cyanide functionalized molecules already found application in polymer electrolytes,[28,29] however, this paper is the first time that enhancement of dielectric properties have been paired with molecular level compatibilization (**Figure 1**). In combination, this leads to a synergistic enhancement of the electromechanical response of a silicone elastomer matrix.

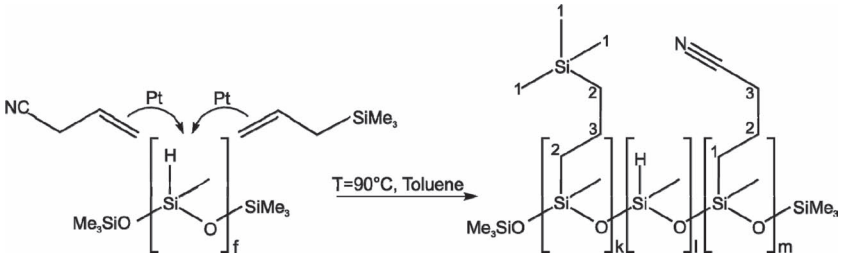

Figure 2. Synthetic pathway of filler molecule CNATS-993. The ratios *k*:*l*:*m* = 0.2:0.1:0.7 were found by ^{1}H NMR spectroscopy. The different proton types are assigned with the numbers to the peaks in Figure 3.

2. Results and Discussion

The filler molecule consists of repeating units of compatibilizer (*k*), unreacted methylhydrosiloxane (*l*) and highly polar cyanides (*m*) (**Figure 2**). The determination of molar ratios between the single groups was carried out via ^{1}H nuclear magnetic resonance (NMR) analysis (**Figure 3**).

The peak at approximately 120 ppm in the ^{13}C NMR spectrum (Figure 3, top) shows clearly the presence of grafted CN-groups in the macromolecule. Not covalently attached CN-groups (mp/bp 120 °C) were evaporated in the synthesis process. The peak at 4.7 ppm (*l*) in the ^{1}H NMR spectrum can be assigned to the single proton of the MeHSiO group by comparison with literature values. Using the other peak positions and the peak areas in the ^{1}H NMR yields a ratio of *k*:*l*:*m* = 0.2:0.1:0.7. This corresponds to 26 units of high dipole moment side-groups ($|\mu|$ = 4.1 D), 7 compatibilizer side-groups covalently attached to the CNATS-993 molecule, and 4 unreacted MeHSiO groups, on average. The four methylhydrosiloxane units that remain in the CNATS-993 molecule could still be used for reactions, however, attempts to form a silicone network with only this molecule as cross-linker were unsuccessful. It is argued that the remaining methylhydrosiloxane units are sterically hindered, so they are blocked from participating

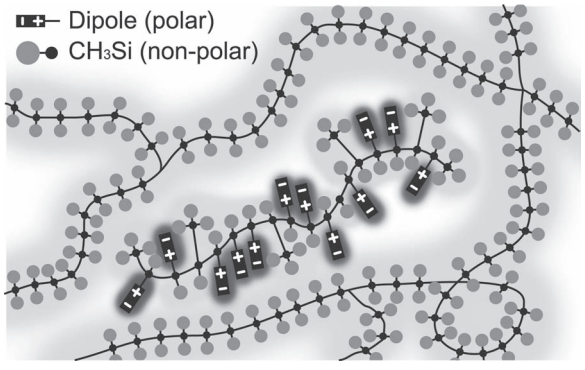

Figure 1. The methylsilane groups (CH_3Si) make the filler, which possesses attached dipoles, compatible with the non-polar host material that consists mainly of dimethylsiloxane units.

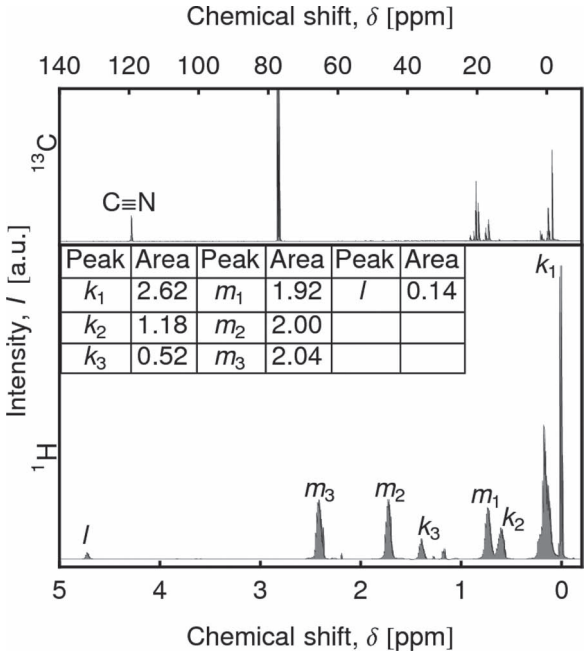

Peak	Area	Peak	Area	Peak	Area
k_1	2.62	m_1	1.92	*l*	0.14
k_2	1.18	m_2	2.00		
k_3	0.52	m_3	2.04		

Figure 3. ^{13}C (top) and ^{1}H NMR (bottom) of allyl-cyano funtionalized filler molecule. The inset table lists all relevant peak areas for structure clarification in the ^{1}H NMR. The peaks *k*, *l* and *m* are assigned to the repeating units of the molecular structure illustrated in Figure 2.

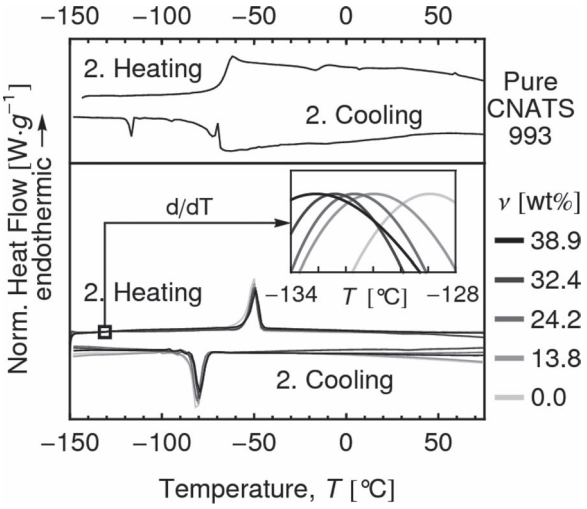

Figure 4. DSC of the pure filler (top) and several silicone films (bottom). The inset magnifies the glass transition region with the first derivative with respect to the temperature *T* to improve reading accuracy.

in further reactions, at least concerning cross-linking reactions or attachment of further side-groups. With the given ratios the molar mass of the product M_{Pr} was calculated as:

$$S_z = \frac{\varepsilon_0 \varepsilon'}{Y} E^2 = \beta E^2 \quad (1)$$

$$M_{pr} = \bar{M} + mf\, M_{AllCN} + kf\, M_{AllSiMe_3} = 4913 \text{ g mol}^{-1} \quad (2)$$

That means that 7.41 g of the isolated product of the filler synthesis correspond to 1.507 mmol, which is almost the complete quantity of the used reactant HMS-993. The allylcyanide groups contribute 35.5 wt% to the total mass of one filler molecule.

DSC was performed (**Figure 4**, bottom) to investigate the influence of the filler molecule on the thermal properties. The inset of Figure 4 shows the first derivative of the second heating curve in the temperature interval from –134 to –128 °C. These curves have a clear maximum, which is typical for the glass transition. For increasing filler content the maxima shift from –129 to –133 °C. This decrease in glass transition temperature is a hallmark of the plasticizing effect.[32] The melting and crystallization peaks at –50 and –80 °C of the second heating and cooling curves, respectively, are typical for silicones.[33] The two curves in the upper graph in Figure 4 represent the second heating and cooling curves for pure CNATS-993. A clear glass transition at –67 °C can be observed for both curves. This transition is not observed with any of the silicone films with CNATS-993, indicating that the filler molecule is well-distributed in the elastomer matrix and does not form individual domains.

The plasticizing effect on the mechanical properties can also be observed with the decreases in Young's modulus (see **Figure 5**) from 900 kPa for the unmodified matrix, down to 250 kPa for the highest CNATS-993 content. This effect is explained by the additional volume of the plasticizer molecule, which effectively decreases the cross-linking density of the silicone network. To substantiate this assumption the well-known formula (Equation 3) is consulted. This equation describes the

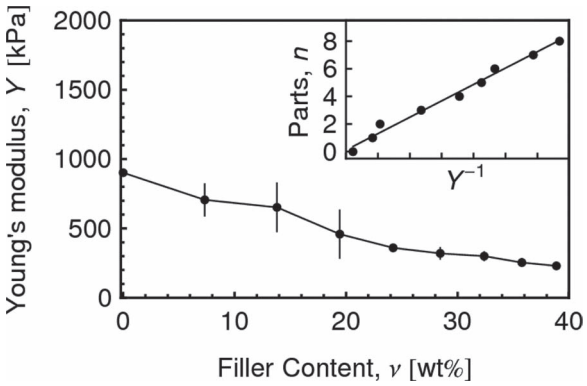

Figure 5. Young's modulus *Y* of allyl-cyano filled silicone films for filler concentrations ranging from 0.0 to 38.9 wt%.

connection between network density *ν*, Young's modulus *Y* and temperature *T* and can be rewritten as Equation 4. Here *R* is the universal gas constant and both *C*s are constants. If the presence of the inert filler has no effect on the cross-linking process of the rubber network, the reduction in stiffness is caused by increase in volume for a constant number of cross-links. Therefore, the dependence of the amount of solution C (Parts *n*) to the inverse Young's modulus should show a linear behavior. This assumption is confirmed by the inset in Figure 5.

$$Y = 3RT\nu \quad (3)$$

$$\Rightarrow n = \frac{C_1}{Y} - C_2 \quad (4)$$

The dielectric relaxation spectroscopy (**Figure 6**) shows an increase in the real part of the permittivity with increasing filler content in the whole frequency range. The enhancement of the dielectric constant can be observed for the whole frequency range. The shifting relaxation peak in the imaginary part of the dielectric constant causes a further increase in permittivity for

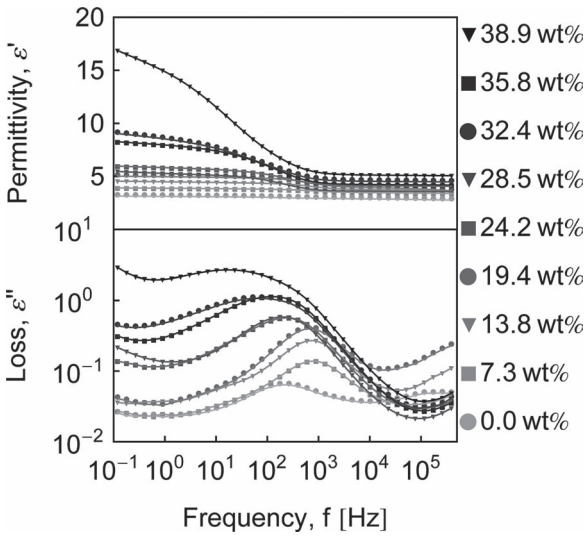

Figure 6. Permittivity spectra of allyl-cyano filled silicone films for filler concentrations ranging from 0.0 to 38.9 wt%.

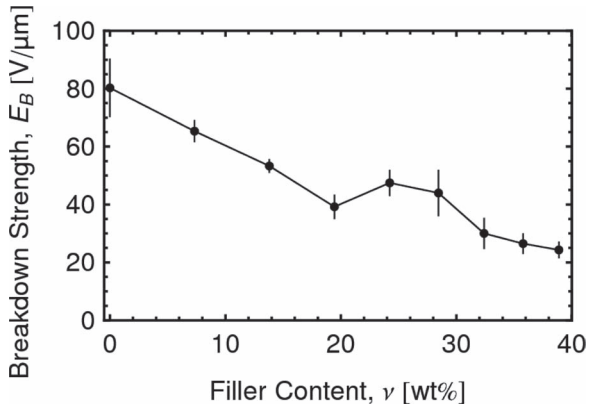

Figure 7. Electrical breakdown strength E_B of allyl-cyano filled silicone films for filler concentrations ranging from 0.0 to 38.9 wt%.

lower frequencies. This relaxation process could be assigned to absorbed water due to the presence of the partial polar filler molecule in the non-polar matrix.

The electrical breakdown (**Figure 7**) decreases with increasing filler concentration from 80 to 20 V μm^{-1}. This is a typical observed behavior for the softening of materials.[9,34] However, this does not exclude this material for DEA applications.

The actuation strain measurements (**Figure 8**) show that the actuation properties change with filler content. As the filler content increases, also the electromechanical response increases. Equation 1 was fitted to the actuation strain curves for small strains to quantify the enhancement of electromechanical response. According to Equation 1, a material with enhanced electromechanical sensitivity β can achieve higher actuation strains for a constant electrical field E. The sensitivity values β are listed in Figure 8, showing a continuous increase with filler content. The sensitivity β is enhanced by a factor 5.5 from 0.0 to 38.9 wt% filler concentration.

3. Conclusions

This paper presents a novel approach in which a filler molecule is functionalized with two different side-groups, one with a high dipole moment and the other with chemical properties similar to the matrix. Several useful material functions and properties are achieved through the use of this functionalized filler: the introduction of side-groups with large dipole moments enhances the permittivity of the silicone, while the mechanical stiffness of the elastomer is lowered by decreasing the network density. The filler molecule shows high compatibility with the elastomer due to the similarity of the nonpolar trimethylsilane side-group to the nonpolar matrix material, ensuring that the filler molecule does not precipitate into separate domains. The filler molecule is inert with respect to the chemistry of the elastomer network formation, and can therefore be added to the reactants during manufacture of the elastomer film. Other strategies for permittivity enhancement of DEA materials, using particles with high dielectric constants,[20–22] are faced with the increase in mechanical stiffness, which in turn leads to negative influence on electromechanical sensitivity. The synergistic combination of property enhancing effects is a strong advantage of this "compatibilized high-permittivity filler" approach. Since the filler molecule improves both mechanical and dielectric behavior, while avoiding complexity in use and ensuring molecular compatibility, it should be possible to employ it in combination with other approaches.

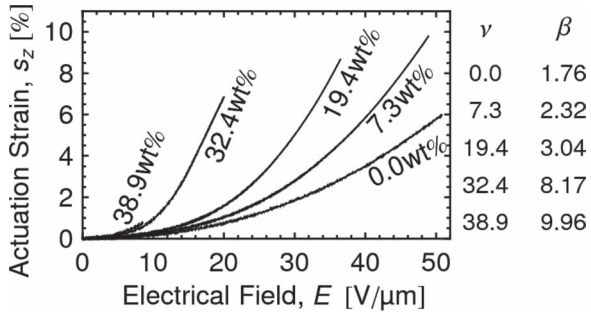

ν	β
0.0	1.76
7.3	2.32
19.4	3.04
32.4	8.17
38.9	9.96

Figure 8. Electrical field dependent actuation strain s_z for filler concentrations ranging from 0.0 to 38.9 wt%. The table (right) shows the weight fraction dependent electromechanical sensitivity β, obtained by fitting Equation 1 to the actuation curves for small strains. [ν] in wt%, [β] = 10^{-3} ×% × V^2 μm^{-2}.

4. Experimental Section

In the following, the synthesis of the elastomer matrix and filler is presented. The chemical characterization and analysis of these materials was performed with NMR and DSC. The dielectric, mechanical and electromechanical properties were also characterized.

Materials: The silicone elastomer matrix consists of vinyl-terminated polydimethylsiloxane (DMS-V41, M = 62 700 gmol^{-1}, Gelest Inc.), reinforced by 15 wt% hexamethyldisilazane-treated silica particles (SIS6962.0, Gelest Inc.). Trimethylsiloxy terminated methylhydrosiloxane–dimethylsiloxane copolymer (HMS-301, M = 1900–2000 gmol^{-1}, x_{MeHSiO} = 25–30 mol%, Gelest Inc.) was used as cross-linker and the reaction was catalyzed using the platinum catalyst "Catalyst EP" (Wacker AG). The filler molecule is based on trimethylsiloxy-terminated polymethylhydrosiloxane (HMS-993, M = 2100–2400 gmol^{-1}, x_{MeHSiO} = 100 mol-%, Gelest Inc.). Allyltrimethylsilane and a platinum complex solution in xylene (2.1–2.4 wt%) were delivered by ABCR, and allylcyanide was purchased by Sigma-Aldrich.

Synthesis of Filler CNATS-993: The molar ratios were calculated based on the average molar mass M = 2250 gmol^{-1} of HMS-993 and the resulting functionality f = 36.92 of the molecule. 3.40 g of HMS-993 (1.51 mmol, 55.75 mmol MeHSiO units) as well as 2.6 mL (16.36 mmol) allyltrimethylsilane and 4.0 mL (49.49 mmol) allylcyanide were dissolved in 100 mL toluene. An excess of allyl components was chosen to ensure high conversions of the MeHSiO units. 0.1 mL of the platinum catalyst solution in xylene was added and the mixture was heated for 22 h at 90 °C under stirring in an argon atmosphere. During the reaction a non-solvable product forms, which was subsequently filtered. All solvable contents were isolated and the solvent as well as remaining allylcyanide and allyltrimethylsilane were evaporated. A yellow oil remains, which was dried overnight in vacuum, leading to 7.41 g of the product CNATS-993 (Figure 2).

Film Preparation: The three solutions were combined in the ratios indicated in **Table 1**. The solutions A and B form the network, and solution C introduces the filler. The solutions were mixed and cast on

Teflon-coated steel substrates, which were confined by metal frames. After solvent evaporation (overnight), the cross-linking reaction is completed by heating to 120 °C for 30 min, forming the final elastomer films. The filler content ν is the mass of filler over the total mass.

Characterization: The filler molecule was characterized with NMR spectroscopy (INOVA500-I500 NMR, Varian) with respect to ^{1}H and ^{13}C atoms. The solvent was deuterated chloroform.

Table 1. Composition of components for preparation of materials.

	Composition
A	26.0 g DMS-V41, 4.6 g SiO_2 particles, 0.2 g Pt catalyst, 123.2 g chloroform
B	1.0 g HMS-301, 40.0 g chloroform
C	7.41 g CNATS-993, 110.61 g chloroform
	Mixing ratio A/B/C = 4:0.5:0 – 8 mL

Thermal properties were investigated with differential scaccing calorimetry (DSC; Diamond DSC, PerkinElmer). Several milligrams of films with 0.0, 13.8, 24.2, 32.4, and 38.9 wt% plasticizer content were cooled down to –150 °C with liquid nitrogen. After a hold time of 4 min at –150 °C, the samples were heated to 75 °C at a heating rate of 20 °C min^{-1}. The cycle was ended with the cooling from 75 to –150 °C. This cycle was repeated to obtain the second heating and cooling curves.

All elastomer films were characterized for mechanical, dielectric, electrical breakdown, and electromechanical properties.

The Young's modulus *Y* was determined using a tensile tester. The films were cut to strips with dimensions 10 mm × 70 mm with a laser cutting system (Versa Laser). These were clamped in the tensile tester (Zwick-Roell, Z005), with a stretchable length of 50 mm. The samples were stretched at constant strain rate of 2.5% s^{-1} until rupture. The Young's modulus

Y was extracted from the slope of the first ten percent of the true stress strain curve.

Electrical breakdown experiments were performed on elastomer disks with a diameter of 12 mm, cut with the laser cutting system. These disks were placed between two spherical metal electrodes. The bottom electrode was positioned to ensure the planar alignment of the sample. The top electrode was fixed with a screw after contacting the surface of the silicone film with a small force. The electrical field between both electrodes was increased at a constant rate of 100 V s^{-1} until electrical failure, with 40 samples for each plasticizer concentration. The expectation value E_B and standard deviation of electrical breakdown strength was estimated based on the Weibull distribution.[30]

The dielectric properties were measured with a dielectric relaxation spectrometer (Alpha-Analyzer, Novocontrol). Electrical contact was ensured with gold powder on both sides of the film (diameter, 20 mm). The real ε' and imaginary part ε'' of the permittivity were measured in a frequency interval from 100 mHz to 100 kHz.

The electromechanical response of the films was investigated using actuators in pure shear configuration. Stiff PET frames were glued with single component silicone (E4, Wacker) to the elastic films. The films were sprayed with a Carbon Black (Printex XE) silicone (Elastosil RT 625, Wacker) mixture dissolved in toluene and hexane to obtain an electroactive region of 70 mm × 10 mm. This yields conductive and compliant electrodes on both sides. To ensure the electrical insulation between both electrodes, 5 mm of each side were covered with a PET mask during the spraying process. After clamping the sample in the tensile tester (Zwick-Roell) and contacting both electrodes to a high voltage source using adhesive aluminum tape, a pre-strain of 10% was applied to the pure shear actuator. After a relaxation time of approximately 1 h, the measurement was started with a constant voltage rate of 5 V s^{-1} in the blocked force mode. The electromechanical sensitivity β was obtained by fitting Equation 1 of Pelrine et al.[31] to the low-field part of actuation strain s_z curves.

Acknowledgements

The authors are grateful for funding from the German government, which was contributed through the German WING program within the NanoFutur-KompAkt (FKZ: 03 × 5511) and PowerAct project (FKZ: 13N10684 and 13N10685). They also thank R. Krause and T. Meissner for help in the laboratories as well as M. Ehlert for performing DSC measurements.

Received: February 2, 2012
Revised: April 23, 2012
Published online: June 8, 2012

[1] Y. Bar-Cohen , *Electroactive Polymer (EAP) Actuators as Artificial Muscles: Reality, Potential, and Challenges*, SPIE Press Monograph, Bellingham, USA **2004.**
[2] M. Blum, *Laser Photonics* **2011**, *3*, 62.
[3] B. F. Grewe, F. F. Voigt, M. van't Hoff, F. Helmchen, *Opt. Express* **2011**, *2*, 2035.
[4] F. Carpi, S. Bauer, D. De Rossi, *Science* **2010**, *330*, 1759.
[5] P. Brochu, Q. Pei, *Macromol. Rapid Commun.* **2010**, *31*, 10.
[6] R. Pelrine, R. Kornbluh, J. Joseph, R. Heydt, Q. Pei, S. Chiba, *Mater. Sci. Eng., C* **2000**, *11*, 89.
[7] R. Pelrine, R. Kornbluh, G. Kofod, *Adv. Mater.* **2000**, *12*, 1223.
[8] X. Zhao, Z. Suo, *Appl. Phys. Lett.* **2007**, *91*, 061921.
[9] M. Kollosche, G. Kofod, *Appl. Phys. Lett.* **2010**, *96*, 071904.
[10] G. Kovacs, P. Lochmatter, M. Wissler, *Smart Mater. Struct.* **2007**, *16*, 306.
[11] M. Niklaus, S. Rosset, H. Shea, *Proc. SPIE Int. Soc. Opt. Eng.* **2010**, 7642.
[12] F. Carpi, G. Frediani, D. De Rossi, *IEEE/ASME Trans. Mechatron.* **2010**, *15*, 308.
[13] M. Aschwanden, M. Beck, A. Stemmer, *IEEE Photonics Technol. Lett.* **2007**, *19*, 1090.
[14] C. Jordi, S. Michel, G. Kovacs, P. Ermanni, *Sens. Actuators, A* **2010**, *161*, 182.
[15] S. Döring, M. Kollosche, T. Rabe, J. Stumpe, G. Kofod, *Adv. Mater.* **2011**, *23*, 4265.
[16] S. Rosset, M. Niklaus, P. Dubois, H. Shea, *Sens. Actuators A* **2008**, *144*, 185.
[17] G. Jordan, D. N. McCarthy, N. N. Schlepple, J. Krissler, H. Schröder, G. Kofod, *IEEE/ASME Trans. Mechatron.* **2011**, *16*, 98.
[18] G. Kofod, D. N. McCarthy, J. Krissler, G. Lang, G. Jordan, *Appl. Phys. Lett.* **2009**, *94*, 202901.
[19] H. Stoyanov, D. N. Mc Carthy, M. Kollosche, G. Kofod, *Appl. Phys. Lett.* **2009**, *94*, 232905.
[20] F. Carpi, D. De Rossi, *IEEE Trans. Dielectr. Electr. Insul.* **2005**, *12*, 835.
[21] G. Gallone, F. Carpi, D. De Rossi, A. Levita, G. Marchetti, *Mater. Sci. Eng. C* **2007**, *27*, 110.
[22] H. Stoyanov, M. Kollosche, S. Risse, D. N. McCarthy, G. Kofod, *Soft Matter* **2011**, *7*, 194.
[23] A. K. Jonscher, *Nature* **1977**, *267*, 673.
[24] F. Carpi, G. Gallone, F. Galantini, D. De Rossi, *Adv. Funct. Mater.* **2008**, *18*, 235.
[25] Q. M. Zhang, H. Li, M. Poh, F. Xia, Z.-Y. Cheng, H. Xu, C. Huang, *Nature* **2002**, *419*, 284.
[26] B. Kussmaul, S. Risse, G. Kofod, R. Wache, M. Wegener, D. N. McCarthy, H. Krüger, R. Gerhard, *Adv. Funct. Mater.* **2011**, *21*, 4589.
[27] D. M. Opris, M. Molberg, C. Walder, Y. S. Ko, B. Fischer, F. A. Nüesch, *Adv. Funct. Mater.* **2011**, *21*, 3531.
[28] I. J. Lee, G. S. Song, W. S. Lee, D. H. Suh, *J. Power Sources* **2003**, *144*, 320.
[29] K. H. Min, D. B. Kim, Y. K. Kang, D. H. Suh, *J. Appl. Polym. Sci.* **2008**, *107*, 1609.
[30] E. Tuncer, D. R. James, I. Sauers, A. R. Ellis, M. O. Pace, *J. Phys. D: Appl. Phys.* **2006**, *39*, 4257.
[31] R. E. Pelrine, R. D. Kornbluh, J. P. Joseph, *Sens. Actuators, A* **1998**, *64*, 77.
[32] E. Jenckel, R. Heusch, *Koll. Z.* **1953**, *130*, 89.
[33] C. E. Weir, W. H. Leser, L. A.Wood, *Rubber Chem. Technol.* **1951**, *24*, 366.
[34] K. H. Stark, C. G. Garton, *Nature* **1955**, *176*, 1225.